stage-specifically in mouse embryogenesis (Fig. 1D). An evolutionarily conserved miRNA such as *mir-1* may have coevolved with its mRNA targets, and hence, could retain a similar developmental or physiological role in diverse taxa (*5*).

lin-4, *let-7*, and the 15 new miRNA genes described here are members of a gene family that could number in the hundreds in *C. elegans* (*18*) and other animals (*19*). To date, approximately 100 miRNA genes have been identified in worms, flies, and human cells (*18, 19*), and it is very likely that the screens conducted so far have not reached saturation. Therefore, additional *C. elegans* miRNAs can be identified using cDNA library sequencing. Also, continued application of whole-genome sequence alignment should identify additional new miRNAs, because this informatics approach complements the cDNA cloning. For example, using only a sample of the worm genome for *C. elegans*/*C. briggsae* alignment, we found two miRNAs (*mir-88* and *mir-89*) that were not represented in the size-selected cDNA library (perhaps due to absent or inefficient processing to the ~22-nt form).

This collection of new miRNAs exhibits a diversity in sequence, structure, abundance, and expression profile. If miRNA genes are as numerous and diverse as they appear to be, they likely occupy a wide variety of regulatory niches, and exert profound and complex effects on gene expression, development, and behavior. The challenge now is to determine the functions of the miRNAs, to identify potential antisense target mRNAs, and to characterize the consequences of their regulatory interactions.

References and Notes

1. V. A. Erdmann *et al.*, *Nucleic Acids Res.* **29**, 189 (2001).
2. R. C. Lee, R. L. Feinbaum, V. Ambros, *Cell* **75**, 843 (1993).
3. B. Reinhart *et al.*, *Nature* **403**, 901 (2000).
4. B. Wightman, I. Ha, G. Ruvkun, *Cell* **75**, 855 (1993).
5. A. E. Pasquinelli *et al.*, *Nature* **408**, 86 (2000).
6. A. Grishok *et al.*, *Cell* **106**, 23 (2001).
7. G. Hutvagner *et al.*, *Science* **293**, 834 (2001).
8. P. A. Sharp, *Genes Dev.* **15**, 485 (2001).
9. Obtained from the ~10% of the *C. briggsae* genome available at the intronerator Web site (www.cse.ucsc.edu/~kent/intronerator/) (*10*).
10. W. J. Kent, A. M. Zahler, *Genome Res.* **10**, 1115 (2000).
11. Using Michael Zuker's mfold (*12*) Web server (http://bioinfo.math.rpi.edu/~mfold/rna/form1.cgi).
12. D. H. Mathews, J. Sabina, M. Zuker, D. H. Turner, *J. Mol. Biol.* **288**, 911 (1999).
13. Supplementary material is available at www.sciencemag.org/cgi/content/full/294/5543/862/DC1.
14. A linker oligonucleotide was ligated to the 3′ end of ~22-nt RNA using RNA ligase, cDNA was prepared by RT-PCR, and the products were cloned in a lambda phage vector (*13*).
15. S. F. Altschul *et al.*, *Nucleic Acids Res.* **25**, 3389 (1997).
16. Sanger Center Ensemble Trace Server (ftp://ftp.ensembl.org/traces/c.briggsae/).
17. Other cDNAs corresponded to *lin-4*, *let-7*, and miscellaneous fragments of ribosomal RNAs, tRNAs, or mRNAs.
18. N. C. Lau, L. P. Lim, E. G. Weinstein, D. P. Bartel, *Science* **294**, 858 (2001).
19. M. Lagos-Quintana, R. Rauhut, W. Lendeckel, T. Tuschl, *Science* **294**, 853 (2001).

20. We thank A. Lee for computer programming, M. McCarthy for worm staging, D. Jewell for helping with BLAST searches, the Sanger Center for *C. briggsae* genomic sequence, and W. J. Kent's Intronerator Web site for presorted worm sequences. We are also grateful to A. Grishok and C. Mello for the *dcr-1* strain and to T. Tuschl and D. Bartel for sharing data prior to publication. This work was supported by NIH grant R01 GM-34028 to V.A.

13 August 2001; accepted 18 September 2001

Single-Molecule Analysis of Chemotactic Signaling in *Dictyostelium* Cells

Masahiro Ueda,[1,6]* Yasushi Sako,[2,6] Toshiki Tanaka,[4]† Peter Devreotes,[5] Toshio Yanagida[3,6]

Single-molecule imaging techniques were used to reveal the binding of individual cyclic adenosine 3′,5′-monophosphate molecules to heterotrimeric guanine nucleotide–binding protein coupled receptors on the surface of living *Dictyostelium discoideum* cells. The binding sites were uniformly distributed and diffused rapidly in the plane of the membrane. The probabilities of individual association and dissociation events were greater for receptors at the anterior end of the cell. Agonist-induced receptor phosphorylation had little effect on any of the monitored properties, whereas G protein coupling influenced the binding kinetics. These observations illustrate the dynamic properties of receptors involved in gradient sensing and suggest that these may be polarized in chemotactic cells.

Chemotaxis, the process by which cells move toward attractant molecules, operates in a range of biological processes including immunity, neuronal patterning, and morphogenesis. *Dictyostelium discoideum* cells display a strong chemotactic response to cyclic adenosine 3′,5′-monophosphate (cAMP), which is mediated by a cell surface receptor and G protein–linked signaling pathway (*1*, *2*). The signaling events downstream of the activated G proteins are initiated locally in the region of the chemotactic cell facing the higher concentration of attractant (cell anterior) even though receptors and G proteins are uniformly distributed on the cell surface (*3–7*). Because the regulatory mechanisms that localize these signaling events are essential for directional sensing (*3*), it is important to reveal the signaling activities of the cAMP receptors and their coupled G proteins in a chemotactic cell.

Recent progress in single-molecule detection techniques has allowed direct monitoring of signaling molecules on the surface of living cells (*8–10*). We extended this technique to real-time imaging of single fluorescent-labeled cAMP molecules bound to their receptors on living *Dictyostelium* amoebae. An orange fluorescent cyanine dye, Cy3, was conjugated to the 2′-OH of the ribose moiety (Cy3-cAMP; Fig. 1A) (*11*). Modification of this position had minimal effects on the binding affinity of the cAMP receptor (*12*), and Cy3-cAMP was functional as a chemoattractant for *Dictyostelium* cells by conventional chemotactic assays (*13*, *14*). The cells exhibited directional movements toward the tip of a micropipette containing 1 μM Cy3-cAMP solution (Fig. 1B). Treatment of cells with Cy3-cAMP or unlabeled cAMP also induced actin polymerization in the cells to a similar extent (*15*). Cy3-cAMP also bound to the cell surface uniformly, similar to the distribution of the cAMP receptors (Fig. 1C) (*4*). Binding of Cy3-cAMP to the cells was inhibited by addition of excess unlabeled cAMP, indicating specific binding of Cy3-cAMP to the cAMP receptors (Fig. 1D).

An objective-type total internal reflection fluorescence microscope (TIRFM) was used to achieve single-molecule imaging of Cy3-cAMP molecules on the basal surface of living cells (*8–10*). When Cy3-cAMP solution (1 nM) was added uniformly to cells, Cy3-

[1]Recognition and Formation, [2]Time's Arrow and Biosignaling, Precursory Research for Embryonic Science and Technology (PRESTO), Japan Science and Technology Corporation (JST). [3]Single Molecule Processes Project, International Cooperative Research Project (ICORP), JST, Mino, Osaka 562-0035, Japan. [4]Biomolecular Engineering Research Institute, Suita, Osaka 565-0874, Japan. [5]Department of Cell Biology, Johns Hopkins Medical Institutions, Baltimore, MD 21205, USA. [6]Department of Physiology and Biosignaling, Graduate School of Medicine, Osaka University, Suita, Osaka 565-0871, Japan.

*To whom correspondence should be addressed. E-mail: ueda@phys1.med.osaka-u.ac.jp

† Present address: Department of Applied Chemistry, Nagoya Institute of Technology, Showa-ku, Nagoya 466-8555, Japan.

cAMP molecules bound to and moved laterally on the basal cell surface (Fig. 2, A and B). Lateral motion allowed distinction between receptor-bound Cy3-cAMP molecules and molecules adsorbed onto the glass slide. To verify that the moving objects were single Cy3-cAMP molecules, we examined the photobleaching characteristics and intensities of the fluorescent spots (*10*). The fluorescence of Cy3-cAMP randomly adsorbed onto a glass surface disappeared in a single step, as expected for photobleaching reactions of a Cy3 molecule attached to cAMP (Fig. 2C). About 73% of moving fluorescent spots on the surface of living cells had fluorescence intensities comparable to those of Cy3-cAMP adsorbed onto the glass surface, indicating that most of moving spots are single molecules of Cy3-cAMP. About 27% of the Cy3-cAMP spots on the surface of living cells had brighter intensities (Fig. 2A, arrowhead). This may represent clusters of Cy3-cAMP–receptor complexes or two or more bound Cy3-cAMP molecules in close proximity on the cell surface. The uneven intensities of the spots representing single molecules were due mainly to fluctuations in fluorescence intensities and variations in distances of the fluorophore from the glass surface (Fig. 2A). Addition of unlabeled cAMP resulted in a decrease in the number of Cy3-cAMP spots. A 50% reduction was achieved with 247 nM cAMP, which is consistent with the previous reports of dissociation constants (*1*, *16*, *17*).

Tracking of individual Cy3-cAMP spots revealed that cAMP-bound receptors were laterally mobile in the plasma membrane (Fig. 2B). Lateral diffusion of the receptor has been suggested by the observation of green fluorescent protein (GFP)–tagged receptors in living amoebae (*4*). The diffusion constant calculated from the motions of individual occupied receptors was about $2.7 \pm 1.1 \times 10^{-10}$ cm^2 s^{-1} ($n = 8$), roughly typical of many membrane proteins including G protein–coupled receptors (*18*). The brighter spots, presumably clusters of the ligand-bound receptors, also moved laterally with a similar diffusion constant. Some of the Cy3-cAMP spots stopped transiently, whereas others moved briefly in a relatively linear path, suggesting possible interactions of occupied receptors with an underlying structure such as cortical cytoskeleton.

Gradients of Cy3-cAMP were formed by adding the Cy3-cAMP solution (0.5 to 1 μM) on an agar sheet as small drops (*19*). In the observed field, cells exhibited linear locomotion toward the source of the Cy3-cAMP (Fig. 3A). Such cells exhibited an elongated shape with an extending pseudopod at the anterior leading edge and a contractile tail at the opposite end, the characteristic morphology of *Dictyostelium* amoebae during chemotaxis. Cells were observed for at least 10 min without any visible signs of damage by laser illumination. There was no specific localization or clustering of bound Cy3-cAMP molecules on the cells undergoing chemotaxis. Receptor occupancy on the anterior half of cells was about 12% greater than on the posterior half of the cell. The lateral diffusion constant of the ligand-bound receptors did not differ between the anterior and posterior halves of the cell.

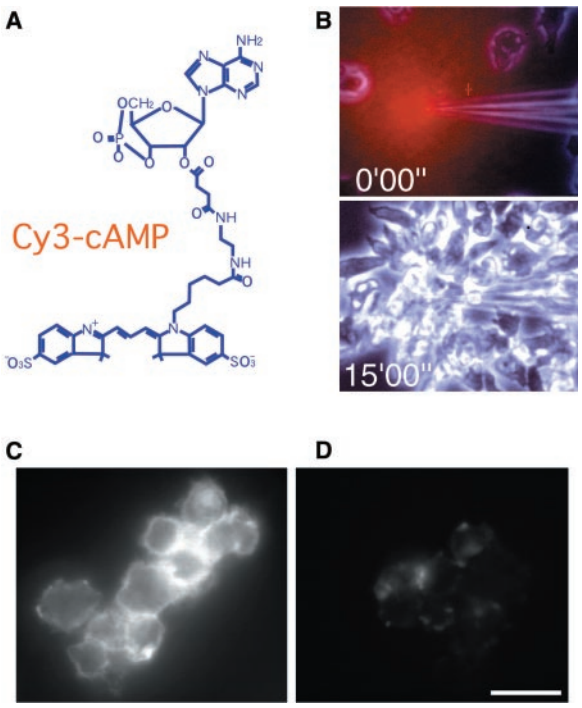

Fig. 1. Chemotactic response of *Dictyostelium* cells to a fluorescent cAMP analog, Cy3-cAMP. (**A**) Structure of Cy3-cAMP. (**B**) Chemotactic response to Cy3-cAMP. The chemotactic assay was performed with a micropipette containing a 1 μM Cy3-cAMP solution. A gradient of Cy3-cAMP was observed with epifluorescence microscopy at the time 0 (red; top). After 15 min of Cy3-cAMP stimulation, the cells accumulated at the tip of the micropipette (bottom). (**C** and **D**) Fluorescence images of Cy3-cAMP bound to *Dictyostelium* cells. The cells were incubated in 10 nM Cy3-cAMP (C) or a mixture of 10 nM Cy3-cAMP and 1 mM unlabeled cAMP (D) and then washed in 98% saturated ammonium sulfate to remove unbound Cy3-cAMP (*12*, *14*). Scale bar, 10 μm.

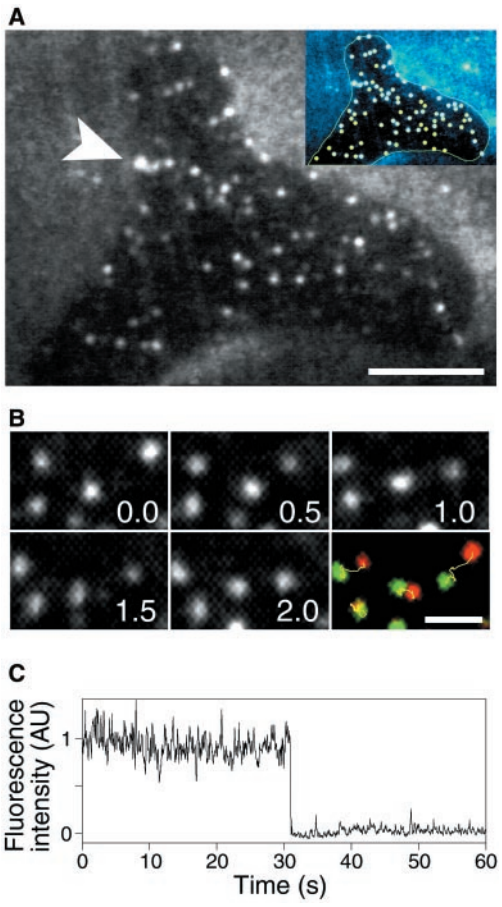

Fig. 2. Single-molecule imaging of Cy3-cAMP on the surface of living *Dictyostelium* cells. (**A**) Cells were observed by objective-type TIRFM (*8*–*10*). Cy3-cAMP solution (1 nM) was added uniformly. (Inset) Superimposed images of the traces of both individual Cy3-cAMP spots (yellow dots) and the cell contour (yellow line). Scale bar, 5 μm. (**B**) Lateral movement of individual Cy3-cAMP–receptor complexes on the cell surface. The color panel represents the merged image of Cy3-cAMP spots at 0 (red) and 2 s (green). Cy3-cAMP spots were linked at 33-ms intervals to show the trajectory (yellow lines). Scale bar, 1 μm. (**C**) An example of a single-step photobleaching event of Cy3-cAMP absorbed randomly onto a glass surface. AU, arbitrary units.

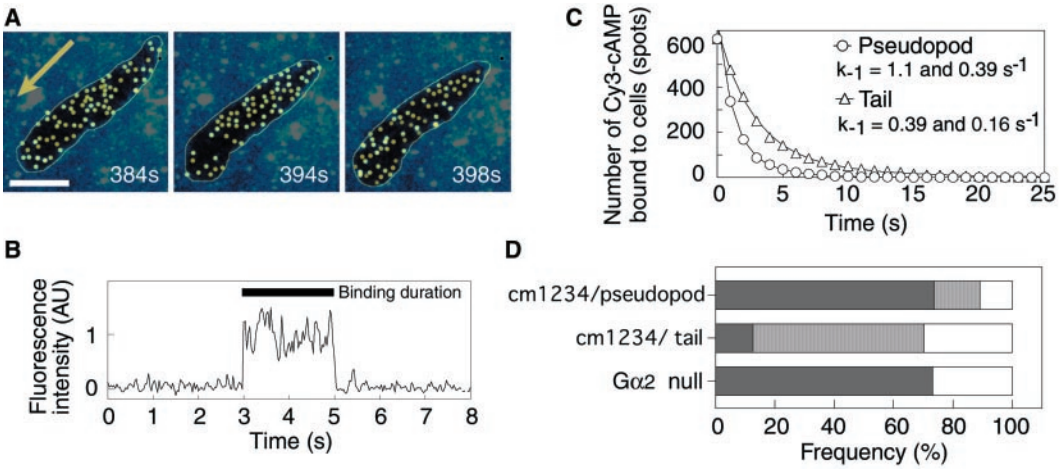

Fig. 3. Single-molecule analysis of the binding kinetics of Cy3-cAMP. (**A**) Receptor occupancy of a *Dictyostelium* cell under a gradient of Cy3-cAMP. Sequential images of the cell were superimposed over the traced image of the individual Cy3-cAMP spots (yellow dots). An arrow indicates the direction of the source of Cy3-cAMP. Time is given in seconds. Scale bar, 10 μm. (**B**) The time course of fluorescence intensity of Cy3-cAMP spots bound to cells, showing disappearance of the fluorescence signal as a single step. (**C**) The release curves of Cy3-cAMP spots bound to the anterior pseudopods (n = 613) or the posterior tails (n = 613). The data were obtained from 10 different cells. The lines represent the fitting of data to a sum of exponential functions. The k_{-1} values indicate the time constants of the fit function. (**D**) Receptor forms in mutant cells. cm1234, a receptor mutant lacking the phosphorylation sites (*17*). $G\alpha_2$ null, a mutant cell lacking G protein α-subunit. In the case of $G\alpha_2$ null cells, the binding data were collected from the entire surface because there are no significant differences in receptor kinetics between pseudopods and tails. The $G\alpha_2$ null cells do not sense a gradient so the front and back of the cells could not be determined with respect to a gradient. The release curves of bound Cy3-cAMP molecules were fitted to three exponentials with k_{-1} = 1.1 s^{-1} (dark gray), k_{-1} = 0.4 s^{-1} (gray), and k_{-1} = 0.16 s^{-1} (white). Correlation coefficients of the fitting are >0.998 in all cases. $cm1234_{anterior}$, n = 501; $cm1234_{posterior}$, n = 484; $G\alpha_2$ null, n = 536.

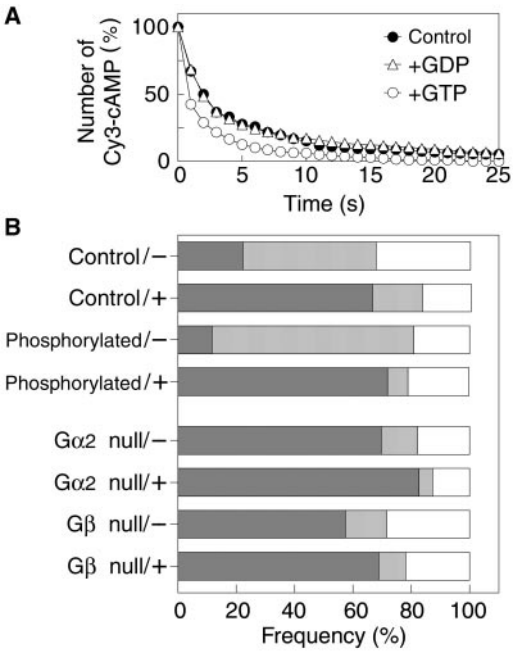

Fig. 4. Single-molecule analysis of the binding kinetics of Cy3-cAMP in membranes. (**A**) The release curves of Cy3-cAMP spots bound to membranes from wild-type cells (*23*). ●, no addition of guanine nucleotides, n = 725; ○, in the presence of 100 μM GTP, n = 709; △, in the presence of 100 μM GDP, n = 730. (**B**) Receptor forms in membranes. The symbols "+" and "−" represent the presence and absence of 100 μM GTP, respectively. The membranes were prepared from the wild-type cells that were pretreated in the absence and presence of cAMP (*17*, *23*). cAMP receptors in these cells are known to be unphosphorylated or phosphorylated, respectively (*17*). For comparison, the release curves were fitted to three exponentials with k_{-1} = 1.3 s^{-1} (dark gray), k_{-1} = 0.4 s^{-1} (gray), and k_{-1} = 0.08 s^{-1} (white). Correlation coefficients of the fitting are >0.998 in all cases. Control/−, n = 725; control/+, n = 709; phosphorylated/−, n = 701; phosphorylated/+, n = 722; $G\alpha_2$ null/−, n = 757; $G\alpha_2$ null/+, n = 659; Gβ null/−, n = 903; Gβ null/+, n = 770.

The kinetics of Cy3-cAMP binding to individual receptors on chemotactic cells was assessed by determining the time difference between the appearance and the disappearance of individual Cy3-cAMP spots on the surface of the cell (Fig. 3B). The majority of the Cy3-cAMP spots disappeared within a few seconds, as expected from the kinetic properties of cAMP receptors (*1*, *20*, *21*). The number of initially present spots remaining in association with the cell as a function of time was determined (Fig. 3C). Cy3-cAMP receptor complexes on anterior pseudopods dissociated faster than those on the posterior tail. These rate differences were observed whether the Cy3-cAMP was applied as a gradient or uniformly, indicating that they derive from an intrinsic cell polarity, rather than being induced by the gradient. The release of bound Cy3-cAMP as a function of time was fitted to sums of exponentials (*22*). At the anterior, 71% of bound Cy3-cAMP dissociated with an exponential rate constant of k_{-1} = 1.1 s^{-1} and 29% with a k_{-1} = 0.39 s^{-1}. At the posterior, 76% had a rate constant k_{-1} = 0.39 s^{-1} and 24% had a rate constant k_{-1} = 0.16 s^{-1}. Previous studies have indicated that the dissociation kinetics of cAMP is multiphasic. Rate constants in these studies were also in the range of $k_{-1} = 1.5^{-1}$ and $k_{-1} = 0.4^{-1}$ (*1*, *20*, *21*). Because steady state amounts of cAMP binding were nearly equal at both ends of the cell, the association rates must also be greater at the anterior end. Thus, the faster cycling of cAMP binding is present at the leading edge pseudopod of the cell.

The difference in the dissociation kinetics between the anterior and the posterior regions of chemotactic *Dictyostelium* cell could be due to receptor phosphorylation, as this modification causes a three- to sixfold decrease in affinity (*17*). Another possibility is altered interactions between the cAMP receptors and downstream signaling molecules components such as heterotrimeric G proteins (*16*). We analyzed a mutant *Dictyostelium* cell expressing cAMP receptors in which the phosphorylation residues were substituted (cm1234) and also a mutant cell lacking the G protein α_2-subunit that couples to the cAMP receptors ($G\alpha_2$ null) (Fig. 3D). Differences in cAMP dissociation kinetics were retained in the cm1234 receptors, indicating that receptor phosphorylation does not cause the observed differences. In contrast, the differences in cAMP dissociation kinetics were absent in cells lacking functional G proteins.

To examine receptor–G protein interactions, the effects of guanosine triphosphate (GTP) on cAMP binding were determined (*23*). In membranes from wild-type cells, GTP induced an increase in the cAMP dissociation rate, whereas guanosine diphosphate (GDP) did not (Fig. 4A). This GTP-dependent decrease in the lifetime of a bound

cAMP molecule was dependent on the presence of G proteins (Fig. 4B). The effects of GTP occurred when receptors were either phosphorylated or not (Fig. 4B). Thus, it is likely that differences in receptor dissociation kinetics result from altered interactions between the receptors and their coupled G proteins rather than receptor phosphorylation. These data are consistent with previous reports indicating that G proteins influence ligand-binding kinetics of the receptors (*16*).

Previous studies of chemotaxis have shown that signaling events are restricted to the leading edge of the cell (*3*–*6*). The differences in the rates of cAMP binding at the front and back of the cell (Fig. 3) resemble the differences in binding to membranes in the presence and absence of GTP, respectively. The faster cycling at the front may indicate that the G protein complex spends less time in an intermediate state associated with receptor before it is activated by GTP and released. Other studies have suggested that such an intermediate state stabilizes agonist binding (*16*, *24*). The receptors at the leading edge also resemble those in the mutant cells lacking G protein, which seems paradoxical but again may indicate that at the cell anterior, the receptor and G protein spend only a short time in the tight association. Although slightly more G protein is present at the anterior (*7*), the more rapid cycling cannot be simply explained by this difference. A property of the membrane or perhaps a regulator of G protein signaling (RGS) protein may facilitate G protein reactivation at the anterior. It will be important to determine how cells initially form such a polarization in receptor states, whether chemoattractant gradients can modify it, and whether it requires interaction with the cytoskeleton.

References and Notes

1. P. M. W. Janssens, P. J. M. Van Haastert, *Microbiol. Rev.* **51**, 396 (1987).
2. C. A. Parent, P. N. Devreotes, *Annu. Rev. Biochem.* **65**, 411 (1996).
3. _____, *Science* **284**, 765 (1999).
4. Z. Xiao, N. Zhang, D. B. Murphy, P. N. Devreotes, *J. Cell Biol.* **139**, 365 (1997).
5. C. A. Parent, B. Blacklock, W. Froehlich, D. B. Murphy, P. N. Devreotes, *Cell* **95**, 81 (1998).
6. R. Meili *et al.*, *EMBO J.* **18**, 2092 (1999).
7. T. Jin, N. Zhang, Y. Long, C. A. Parent, P. N. Devreotes, *Science* **287**, 1034 (2000).
8. A. Ishijima, T. Yanagida, *Trends Biochem. Sci.* **26**, 438 (2001).
9. M. Tokunaga *et al.*, *Biochem. Biophys. Res. Commun.* **235**, 47 (1997).
10. Y. Sako, S. Minoguchi, T. Yanagida, *Nature Cell Biol.* **2**, 168 (2000).
11. Supplementary Web material (Method of Cy3-cAMP preparation) is available on *Science* Online at www.sciencemag.org/cgi/content/full/294/5543/864/DC1.
12. P. J. M. Van Haastert, E. Kien, *J. Biol. Chem.* **258**, 9636 (1983).
13. T. M. Konijn, P. J. M. Van Haastert, *Methods Cell Biol.* **28**, 283 (1987).
14. P. N. Devreotes *et al.*, *Methods Cell Biol.* **28**, 299 (1987).
15. Chemoattractant-induced F-actin formation was measured as described [A. L. Hall, A. Schlein, J. Condeelis, *J. Cell Biochem.* **37**, 285 (1988)]. The amount of F-actin increased biphasically with two peaks (at 10 s and at 60 to 100 s) by addition of Cy3-cAMP.
16. L. Wu, R. Valkema, P. J. M. Van Haastert, P. N. Devreotes, *J. Cell Biol.* **129**, 1667 (1995).
17. Z. Xiao, Y. Yao, Y. Long, P. N. Devreotes, *J. Biol. Chem.* **274**, 1440 (1999).
18. D. A. Jans, *Biochem. Biophys. Acta* **1113**, 271 (1992).
19. *Dictyostelium discoideum* cells (strain AX2) were cultured axenically with standard culture techniques (*25*). Cells were starved in Sörensen's phosphate buffer (14.6 mM KH_2PO_4, 2 mM Na_2HPO_4, pH 6.0) for 6 hours and then treated with 5 mM caffeine for 30 min to inhibit adenylate cyclase (*14*). After the cells were suspended in the buffer supplemented with 2 mM $MgSO_4$, 5 mM caffeine, and 1 mM dithiothreitol (DTT), an aliquot was placed on a glass cover slip and covered with a thin agarose sheet (*26*). For the chemotactic assay, a small droplet of Cy3-cAMP solution (0.5 to 1 μM) was placed on the agar sheet. The cells in the field of about 1 to 2 mm away from the droplet of Cy3-cAMP were observed.
20. P. J. M. Van Haastert, R. J. W. de Wit, *J. Biol. Chem.* **259**, 13321 (1984).
21. _____, P. M. Janssens, F. Kesbeke, J. DeGoede, *J. Biol. Chem.* **261**, 6904 (1986).
22. The anterior pseudopods or the posterior tails are defined as regions within 10 μm from the leading edge or the rear end of a cell, respectively. The release curves of bound Cy3-cAMP molecules were fitted to the sums of exponentials by the least squares methods with the Levenberg-Marquardt algorithm (KaleidaGraph; Hulinks). The fit was executed for two, three, or four exponentials, because kinetic analysis of cAMP binding to the cells reveals four different forms of its receptors (*1*, *20*, *21*).
23. Membranes were prepared as described (*21*). The wild-type (AX2) and mutant cells in Sörensen's buffer were pretreated for 30 min with either 5 mM caffeine or 10 mM DTT plus 10 μM cAMP to convert the receptors into either the unphosphorylated or phosphorylated states, respectively (*17*). The cells were broken by passing them through a Millipore filter (pore size, 5 μm). After centrifugation of the homogenates, the pellet was collected and resuspended in 10^8 cell equivalents per milliliter in Sörensen's buffer supplemented with 2 mM $MgSO_4$. An aliquot of the suspension was placed on a glass cover slip for 30 min on ice. After washing with the buffer, Cy3-cAMP solution (10 nM) was added. The $G\alpha_2$ null and Gβ null cell lines used in this study are JM1 and LW14, respectively (*16*).
24. A. Levitzki, I. Marbach, A. Bar-Sinai, *Life Sci.* **52**, 2093 (1993).
25. M. Claviez *et al.*, *EMBO J.* **1**, 1017 (1982).
26. S. Yumura, H, Mori, Y. Fukui, *J. Cell Biol.* **99**, 894 (1984).

27. We thank J. West and F. Brozovich for critical reading of the manuscript and our colleagues of the Single-Molecular Processes Project for valuable discussion.

29 June 2001; accepted 31 August 2001

Recruitment of Mec1 and Ddc1 Checkpoint Proteins to Double-Strand Breaks Through Distinct Mechanisms

Tae Kondo,[1]* Tatsushi Wakayama,[1]* Takahiro Naiki,[1]* Kunihiro Matsumoto,[1,2] Katsunori Sugimoto[1]†

In response to DNA damage, eukaryotic cells activate checkpoint pathways that arrest cell cycle progression and induce the expression of genes required for DNA repair. In budding yeast, the homothallic switching (HO) endonuclease creates a site-specific double-strand break at the mating type (*MAT*) locus. Continuous *HO* expression results in the phosphorylation of Rad53, which is dependent on products of the ataxia telangiectasia mutated–related *MEC1* gene and other checkpoint genes, including *DDC1*, *RAD9*, and *RAD24*. Chromatin immunoprecipitation experiments revealed that the Ddc1 protein associates with a region near the *MAT* locus after *HO* expression. Ddc1 association required Rad24 but not Mec1 or Rad9. Mec1 also associated with a region near the cleavage site after *HO* expression, but this association is independent of Ddc1, Rad9, and Rad24. Thus, Mec1 and Ddc1 are recruited independently to sites of DNA damage, suggesting the existence of two separate mechanisms involved in recognition of DNA damage.

When DNA is damaged, cells activate a response pathway that arrests the cell cycle and induces the transcription of genes that facilitate repair. The failure of this response results in genomic instability that may lead to cancer in higher eukaryotes (*1*). The systems that monitor the structure of the chromosomes and coordinate repair and cell-cycle progression are termed "checkpoints" in eukaryotic cells. In budding yeast, two essential genes, *MEC1* and *RAD53*, form the core of the DNA damage checkpoint pathway (*2*, *3*). Mec1 belongs to a superfamily of large protein kinases, including human ATM and ATM-

[1]Division of Biological Science, Graduate School of Science, Nagoya University, [2]CREST, Japan Science and Technology Corporation, Chikusa-ku, Nagoya 464-0814, Japan.

*These authors contributed equally to this work.
†To whom correspondence should be addressed. E-mail: j46036a@nucc.cc.nagoya-u.ac.jp